Vol. 374: 181–198, 2009
doi: 10.3354/meps07761

MARINE ECOLOGY PROGRESS SERIES
Mar Ecol Prog Ser

Published January 13

Response of small copepods to an iron-induced phytoplankton bloom: a model to address the mechanisms of aggregation

S. Krägefsky*, U. Bathmann, V. Strass, D. Wolf-Gladrow

Alfred Wegener Institute for Polar and Marine Research, Am Handelshafen 12, 27570 Bremerhaven, Germany

ABSTRACT: We investigated the causes of a large increase in abundance of small copepods, in particular *Oithona similis*, that was observed during the iron fertilisation experiment EisenEx in the Southern Ocean. *Oithona* spp. individuals showed a pronounced migratory response and shifted their vertical distribution towards the progressively phytoplankton-enriched surface layer in the bloom area, while outside, in the area with dilute food concentration, a substantial number of individuals resided in deeper layers. This deep-dwelling behaviour affected an increased drift relative to scarce food in the surface layer, whereas upward migration led to a gradual accumulation of animals in the bloom area. Our simulation study takes into account the particular flow field and the migratory response of *Oithona* spp. and shows that it can explain most of the abundance increase in *Oithona* spp. observed during EisenEx. The migratory behaviour of *Oithona* spp. may be considered as a food-finding strategy to cope with the patchy, mostly poor food environment of the Southern Ocean.

KEY WORDS: Copepod aggregation · *Oithona* spp. · Southern Ocean · Iron fertilisation · Vertical migration · Oceanic flow field · Food-finding strategy

INTRODUCTION

Ocean currents of different spatiotemporal scales keep pelagic organisms in permanent motion. Some currents are short transient features; other circulation patterns like mesoscale eddies and meanders last for weeks or months. Large-scale, persistent currents are part of the global ocean circulation, of which the Antarctic Circumpolar Current (ACC) has the largest transport (≈130 Sv). Current speeds within the ACC can exceed 0.5 m s^{-1}.

The ACC governs the circulation of the Southern Ocean, which is the largest high nutrient–low chlorophyll (HNLC) region on earth. The phytoplankton production is strongly limited by low iron availability (Boyd et al. 2007). Blooms of large phytoplankton, whose occurrence is regionally and seasonally restricted, strongly increase phytoplankton biomass locally above the background of pico- and nanophytoplankton (Smetacek et al. 1990). These typically are mesoscale blooms and develop and decay on the time scale of weeks (Moore & Abbott 2002).

Total metazoan biomass in the Southern Ocean is dominated by copepods (Voronina 1998), whose life cycles are on the order of several months to years in this environment (Atkinson 1998, Schnack-Schiel 2001). Single phytoplankton blooms thus cover a short fraction of their generation times.

Copepods feature swimming speeds up to many body lengths per second, but still drift with the ocean currents without the ability to move against them by own horizontal movements. Vertical differences in the oceanic flow field cause a depth dependency of their drift, and vertical movements may cause significant changes in drift direction and speed.

There is increasing evidence that copepods and various other planktonic animals are able to utilise these differences to maintain their horizontal distribution or to move in a certain direction by means of their vertical migration (Bosch & Taylor 1973, Peterson et al. 1978,

*Email: soeren.kraegefsky@awi.de

Kimmerer & McKinnon 1987, Batchelder et al. 2002, Emsley et al. 2005). Vertical migration also increases or decreases the drift divergence between organisms or particles located at different depth, e.g. between migrating copepods and food items in the surface layer.

Hardy & Gunther (1935) raised this topic for the first time to explain an anti-correlated spatial distribution of phytoplankton and crustaceans found during the 'Discovery' expedition 1926–1927 to the South Georgia whaling grounds. They hypothesised an exclusion of crustacean zooplankton from phytoplankton-rich areas due to an increased drift divergence induced by an active avoidance of phytoplankton dense layers. In contrast to the supposed avoidance behaviour, however, copepods and other crustacean were attracted by abundant phytoplankton in the verification experiments done by Bainbridge (1953), whose findings thus reverse the exclusion hypothesis.

Mesoscale iron fertilisation during *in situ* experiments induced mesoscale phytoplankton blooms in HNLC areas. During 6 of 12 experiments a rise in the abundance of copepods was observed in the bloom areas. The experiments covered observation periods of 5 to 37 d, and were conducted under different abiotic conditions (Boyd et al. 2007).

During 2 iron fertilisation experiments in the ACC, EisenEx (Cisewski et al. 2005) and EIFEX (Strass et al. 2005), the experimental set-up provided nearly ideal conditions for surveying the response of copepods and other zooplankton to the experimentally raised food concentration in the fertilised patch. Both experiments were conducted within the nearly closed circulation of a mesoscale eddy. Hence, over the course of the experiments the zooplankton within the experimental area remained nearly unaffected by an exchange with zooplankton from adjacent water.

During these fertilisation experiments, an increase of up to 2–3 times in the abundance of diurnally and non-diurnal vertical migrating copepods was detected inside the phytoplankton bloom area over the course of the experiments (Henjes et al. 2007, S. Krägefsky unpubl. data). The aim of this model study is to explore the impact of the observed migratory response of non-diurnal migrating copepods in different flow fields. The following questions are addressed: whether and to what extent do copepods utilise vertical differences in current speed and direction to increase their food gain.

MODEL DESCRIPTION

A Lagrangian individual-based model (IBM) is used to track copepods. These copepods are exposed to different flow regimes, which are simplified representations of those at the experimental site during EisenEx and EIFEX. Individuals in the model are representative of a number of neighbouring copepods in the field. Their motional behaviour is prescribed to force a characteristic vertical distribution of copepods outside and a gradual vertical redistribution inside a bloom area accordant to the field findings during EisenEx. Basically, it forced an upward migration of individuals towards the progressively food-enriched surface layer.

The simulations account for the migratory response of adults and copepodites of the genus *Oithona* spp., in particular *Oithona similis*, which clearly dominated the fraction of small-sized copepods in terms of abundance and biomass during EisenEx and EIFEX (Henjes et al. 2007). Their stage-specific development, which was observed over the course of these experiments, indicates no advanced recruitment into and within copepodite stages inside the bloom areas (Wend 2005). Consequently, the simulations do not account for copepod growth and mortality. The model study assesses the magnitude of changes in horizontal copepod distribution as solely caused by directional vertical migration of copepod individuals, drifting in a vertical sheared flow field (Fig. 1).

The path followed by a copepod individual (i) at location $\vec{X}_i$ is given by:

$$\frac{d\vec{X}_i}{dt} = \vec{U}_i \quad (1)$$

where t is time. $\vec{U}_i$, the actual velocity of a copepod, results from superposition of directional ($\vec{u}_{d_i}$) and random ($\vec{u}_{r_i}$) copepod motion and copepod drift with ocean currents ($\vec{u}_{m_i}$).

$$\vec{U}_i = \vec{u}_{d_i} + \vec{u}_{r_i} + \vec{u}_{m_i} \quad (2)$$

Subscript i, which denotes a single copepod, is dropped in the following. The active motion is assumed to be at a constant speed V_A. Its vertical directionality is determined by the attraction factor g_z, within a value range of −1 (moving upward at speed V_A) and 1 (moving downward at speed V_A) (see 'Directionality of copepod motion'):

$$\vec{u}_d = \begin{pmatrix} 0 \\ 0 \\ V_A g_z \end{pmatrix} \quad (3)$$

The active motion includes an isotropically distributed random component. Its share is reduced by the copepod's directionality:

$$\vec{u}_r = \begin{pmatrix} V_A(1-|g_z|)\sin(\delta)\cos(\varphi) \\ V_A(1-|g_z|)\sin(\delta)\sin(\varphi) \\ V_A(1-|g_z|)\cos(\delta) \end{pmatrix} \quad (4)$$

The angles $\delta(0 \le \delta \le \pi)$ and $\varphi(0 \le \varphi < 2\pi)$ are chosen randomly at each time step. If $R(0, 1)$ is a random variable of uniform distribution on the unit interval, φ and δ are given by $\varphi = 2\pi R(0, 1)$ and $\delta = \arccos[1-2R(0, 1)]$, respectively.

Copepod individuals drift with horizontal currents, their respective drift velocity is given by:

$$\vec{u}_m = \begin{pmatrix} u_s + u_{im} \\ v_{im} \\ 0 \end{pmatrix} \quad (5)$$

Copepod drift is determined by stationary flow (u_s) and flow components due to inertial oscillations (u_{im} and v_{im}). Given the copepods' ability to maintain their position or to swim against vertical currents and mixing, we did not account for these vertical components of the flow field, for simplicity (see 'Flow field and model geometry').

Directionality of copepod motion

Motional behaviour of copepod individuals affects prey perception and likewise their own conspicuousness. It is thus essentially linked to food gathering and predator avoidance (Tiselius & Jonsson 1990, Kaartvedt et al. 1996). Motion of a copepod individual in the model represents the displacement of the centre of mass of a number of neighbouring copepods in the field. It is assumed that this displacement is directional within a stimuli gradient due to frequent movements of individuals towards (or away from) the stimuli.

We abstract from the particular predator avoidance and foraging behaviour of individual copepods, which are addressed by other copepod IBM studies (Wiggert et al. 2005, Woodson et al. 2007). Formulation of the motional behaviour of individuals thus has a descriptive character. It forces the observed redistribution of *Oithona* spp. within the bloom area during EisenEx and may help to explain the absence of pronounced vertical redistribution during EIFEX.

During EisenEx a net upward migration of individuals towards and redistribution within the progressively food-enriched surface layer led to an increasingly correlated depth distribution of *Oithona* spp. with microzooplankton and diatoms. Correlation between *Oithona* spp. and microzooplankton declined after the middle of the experiment with diminishing abundance of a fraction of microzooplankton (e.g. dinoflagellates), which initially had increased during EisenEx (Henjes et al. 2007). In contrast, after its increase the correlation between diatom and *Oithona* spp. depth distribution stayed constant at high values inside the fertilized patch, while there was a weak to moderate correlation in the non-fertilised area throughout the experiment (see Fig. 2).

Microzooplankton may have remained an important fraction of the diet of *Oithona* spp. still in the bloom situation throughout the experiment (see 'Discussion'). However, exclusive use of diatoms as trigger of the local attraction of *Oithona* spp. individuals seems to be appropriate for the model purpose.

Repulsion of *Oithona* spp. is supposed to be caused by other *Oithona* spp. individuals and by an avoidance of the near surface layer. Attraction and repulsion of copepods is defined by the field Φ as a function of diatom carbon concentration (F; Eq. 10), local copepod density (ρ_{zoo}) and residence depth (z), as:

$$\Phi(x, y, z, t) = \alpha F - \beta \rho_{zoo} - \gamma e^{-z/z_a} \quad (6)$$

where α is the food attraction coefficient, β is the repulsion coefficient, γ is the surface avoidance coefficient and (e^{-z/z_a}) is an exponential declining quantity, where z_a is the decaying length.

Attraction by diatoms

The remote prey perception ability of *Oithona* spp. is assumed to be biased towards larger immobile particles and motile prey (Visser 2001). The floristic shift towards large diatoms, which happened during EisenEx and other iron fertilisation experiments, thus, likely had potentiated attraction by diatoms. For the sake of simplicity, however, no size-dependent attraction is introduced in the model, but is assumed to be proportional to the local diatom carbon concentration (F). Its attraction is weighted by the attraction coefficient α (Eq. 6) (see 'Diatom distribution').

Surface avoidance

The vertical field distribution of *Oithona* spp. further indicates an avoidance of the near surface layer. With this behaviour *Oithona* spp. may reduce the risk of visual predation and avoid a high-turbulence environment which affects their prey perception (Maar et al. 2006). Light, and thus visibility, and in many cases near surface turbulence, decays exponentially with depth (Anis & Moum 1995). Accordingly, we prescribe surface avoidance in general form by an exponential declining quantity (e^{-z/z_a}) that is determined by the decay length z_a, independent of the actual light field and temporal changes inside the fertilised patch. We assume a constant $z_a = 10$ m; thus, the quantity is 1 at the surface, decays to about 0.5 at 7 m depth and is less than 0.15 at 20 m. Surface avoidance is weighted by the surface avoidance coefficient γ (Eq. 6).

Repulsion due to other individuals

Like other copepods, *Oithona* spp. individuals possess a sensitive remote sensing ability. They use hydromechanic signals to detect prey and predators (Svensen & Kiørboe 2000). We assume that the presence of other individuals causes hydromechanic disturbances that potentially mask prey signals and may induce escape reactions. Predominance of hydromechanic disturbances should effect a net repulsion of animals out of a local volume and thus act to disperse individuals within the water column. We introduce a repulsion term assuming proportionality to the local *Oithona* spp. density (ρ_{zoo}) and weight the repulsive effects by the repulsion coefficient β (Eq. 6).

A model individual represents an invariant number of neighbouring copepods in the field (N_{oit} l^{-1}) within the range $\pm dx/2$, $\pm dy/2$ and $\pm dz/2$ around its actual position. Model individuals are initially uniformly distributed (ρ_o), and N_{oit} l^{-1} corresponds to the mean *Oithona* spp. density in the field within the depth range covered by the model domain (0 to 160 m). During EisenEx the corresponding *Oithona* spp. density was 9 ind. l^{-1} including adults and copepodites in the non-fertilised area.

For the purpose of generalization, dependency on the actual field abundance is dropped and ρ_{zoo} is given as relative abundance by use of the initial abundance (ρ_o) as reference. Thus, the local copepod density initially is $\rho_{zoo} = 1$ throughout the model domain.

Attraction factor g_z

Net directional displacement of copepod individuals which are located in a small volume with a vertical gradient of attractive or repulsive stimuli is assumed to be along or against the gradient, respectively. The horizontal components of the gradient of Φ, which defines local attraction or repulsion in our model (Eq. 6), are much smaller than the vertical component, and are neglected. The vertical component $\partial\Phi/\partial z$ is used to define the attraction factor g_z, which by use of the hyperbolic tangent function is limited to the range of –1 to 1.

$$g_z(x,y,z,t) = \tanh\left(\frac{\varepsilon\partial\Phi}{2\partial z}\right) \quad (7)$$

The attraction factor g_z forces a directional up- or downward motion of copepod individuals in the model and proportionally reduces the share of random motion ($\vec{u}_r$) (see Eqs. 3 & 4). The constant scaling parameter ($\varepsilon = 10$) determines the slope of the response curve and is chosen arbitrarily.

Swimming speed

Actual activity of neighbouring copepods covers different patterns of motion. In feeding experiments *Oithona similis* showed low sinking of the order of 0.1 mm s^{-1} and rapid escape and food gathering jumps at a velocity of ~14 mm s^{-1} (Svensen & Kiørboe 2000). Accounting for the low frequency of jumps (~8 jumps min^{-1}) and jump length (~2 mm), the observed motion (sinking and jumping) equates to a nominal speed of about 0.4 mm s^{-1}. Uchima & Hirano (1988) found a nominal swimming speed of *O. davisae* of roughly 0.7 mm s^{-1}, e.g. leaping and paddling forward. Activity may be higher in the stimuli-rich oceanic environment. Nevertheless, we assume slow constant motion of the model individuals at speed V_A in the range of 0.5 to 1 mm s^{-1}, during different model runs.

Flow field and model geometry

The flow field at the experimental site during EisenEx and EIFEX was governed by the quasi-steady geostrophic eddy circulation. Superimposed fluctuations were mainly associated with tides and inertial oscillations. During both experiments the patch with the iron-induced diatom bloom circled around the eddy centre. Under the assumption of an ideal symmetric eddy circulation, the copepod drift in relation to the bloom patch is accurately modelled within a channel flow.

Stationary flow along the channel is defined by means of geostrophic velocity profiles derived from deep CTD-profiles (conductivity temperature and depth probe) measured during EisenEx. During EIFEX, measurements with an acoustic Doppler current profiler (ADCP) attached to a buoy, which was drifting with the fertilised patch, provided direct measurements of the vertical shear of the flow field along its path. Measurements were low-pass filtered to remove tidal components and fluctuations caused by inertial oscillations. The depth-dependent stationary flow in the x-direction, $u_s(z)$, is defined using the mean velocity magnitude of residual flow in the EIFEX case, while the stationary flow in y and z directions, v_s and w_s, are zero (Fig. 1a).

Flow fluctuations superimposed on the stationary flow field are taken into account by defining an idealised inertial motion:

$$u_{im}(z,t) = V_H \times \sin\left[2\Omega\sin\left(\frac{2\pi}{360}\times \mathrm{lat}\right)\times t\right] \times\{0.5 - 0.5\times\tanh[h_t^{-1}(z - z_{mt})]\} \quad (8)$$

and

$$v_{im}(z,t) = V_H \times \cos\left[2\Omega\sin\left(\frac{2\pi}{360}\times \mathrm{lat}\right)\times t\right] \times\{0.5 - 0.5\times\tanh[h_t^{-1}(z - z_{mt})]\} \quad (9)$$

The respective time-dependent velocity components at the surface are given by the velocity amplitude, V_H, and the second factor of the equation. The third factor defines the depth dependency, where h_t is the slope factor and z_{mt} is the depth of the mixed layer (Table 1).

The drift of copepod individuals is treated as a movement relative to the upper patch centre, which is fixed in the model runs. The patch centre is located at the middle of the channel-like model domain. The model domain is bounded by the vertical planes $-by$ and $+by$ along the channel and by $-bx$ and $+bx$ perpendicular to it (Fig. 1b). In- and outflow conditions of copepod individuals at these boundaries are defined as follows.

Table 1. Definitions and parameter range

Parameter	Definition	Units	Value
V_H	Velocity amplitude of inertial oscillation	m s^{-1}	0.2
V_A	Swimming speed of copepod	m s^{-1}	0.0005–0.001
Ω	Angular velocity of rotation of earth	rad s^{-1}	7.29×10^{-5}
lat	Latitude	°	–48
h_t	Slope factor	m	15
z_{mt}	Mixed layer depth	m	20–120
Z_{max}	Vertical extent of the model domain	m	160
τ	Dilution time scale	d	10
α	Food attraction coefficient	$m^2\ s^{-2}\ \mu M^{-1}$	0.5–8
β	Repulsion coefficient	$m^2\ s^{-2}$	0–4
γ	Surface avoidance coefficient	$m^2\ s^{-2}$	1–2
ε	Scaling factor	$m^{-1}\ s^{-2}$	10
z_a	Decay length	m	10
δ	Zenith	rad	0–π
φ	Azimuth	rad	0–2π

Drift differences on the order of km d^{-1} between deep-dwelling copepods and the phytoplankton patch within the surface layer are comparatively moderate in proportion to the length of the patch trajectory around the eddy centre (in the range of 200 to 300 km). Despite circular trajectories in the eddy flow field, deep-dwelling individuals did not drift a second time into the bloom area within the time frame of the experiments. For modelling purposes, there is thus no need to track the path of copepod individuals outside the area covered by the model domain. Individuals permanently leave the model domain at the boundaries $-bx$ and $+bx$.

Inflow of individuals into the model domain has to sustain a characteristic outpatch distribution of copepods, which ensures a characteristic flow of deep-dwelling copepods towards the bloom area. It rises gradually during the simulation and corresponds to a dynamic equilibrium of repulsive and attractive effects (see 'Model sensitivity').

A steady state distribution develops during an initialisation period as a result of vertical migration of inward-drifting copepods, which initially pass through an area with permanently low diatom concentration. Depending on direction of the stationary flow (u_s), the respective areas are left to $-bx_e$ or right to $+bx_e$. These are inner planes at which we sample the actual inward flow of copepod individuals. A correspondent actual inflow of new individuals into the model domain is forced at the outer boundary $-bx$ or $+bx$, respectively.

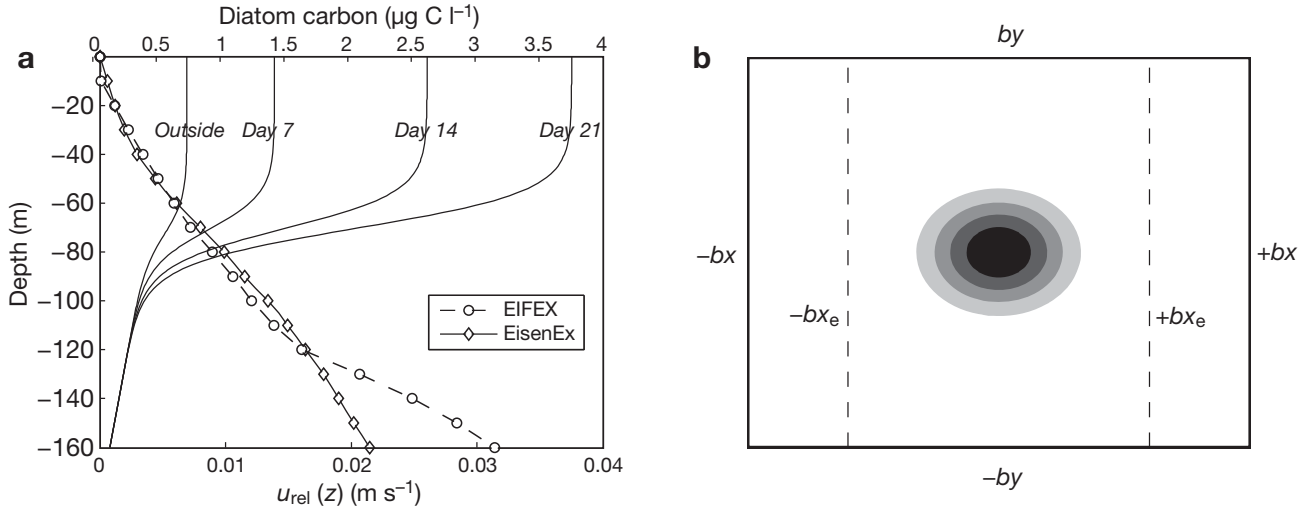

Fig. 1. (a) Profiles of the carbon concentration outside the bloom area and at Days 7, 14 and 21 inside the bloom area (solid lines) and depth-dependent drift velocity of copepods relative to the upper patch centre, $u_{rel}(z)$. EIFEX and EisenEx: iron fertilisation experiments. (b) Sketch of the model domain with the outer boundaries $-bx$, $+bx$, $-by$ and $+bx$ and the inner planes $-bx_e$ and $+bx_e$; grey-black shadings mark the diatom carbon concentration (black marks the highest concentration)

It keeps recent changes in copepod distribution and allows for further changes during the drift of new individuals passing through the area.

The flow component that determines the copepod drift ($\vec{u}_m$) in the y-direction is oscillatory or zero, if we account for inertial motion (Eq. 9) or not, respectively. Individuals which exit at $-by$ or $+by$ are wrapped around and enter the model domain at the opposite side.

Diatom distribution

Diatom stock is not a prognostic variable in the model. The simulated diatom distribution follows the observed progression in the field (Assmy et al. 2007), but with the following simplifications: In the horizontal model plane the bloom area has a circular or elliptical shape. We omit small-scale field variability and assume a horizontal bell-shaped diatom distribution. For the vertical, we assume a uniform distribution in the mixed layer and a sharp decline in concentration below.

The diatom distribution (F) is given in terms of diatom carbon concentration (µmol C l^{-1}):

$$F(x,y,z,t) = \{C_0 + [C_s(t) - C_0] \times f_h\} \times f_v + C_{sub} \quad (10)$$

In this equation C_0 = 0.74 µmol C l^{-1} is the surface diatom carbon concentration in the non-fertilised area. The time-dependent diatom carbon concentration at the patch centre $C_s(t)$ follows the increase of its mean concentration in the upper 50 m over the course of EisenEx (Fig. 1a).

The horizontal pattern of diatom distribution is determined by f_h, specifying a bell-shaped distribution:

$$f_h = e^{-\frac{\pi^2}{2}\left(\frac{x^2}{a^2} + \frac{y^2}{b^2}\right)} \quad (11)$$

The semi-major axis, half of the longest ellipse diameter a, and semi-minor axis, b, give the extent of the bloom area, which increases in time. Simulating a circular bloom area ($a = b$), these are equal to the patch radius, $r_p(t)$ (Eq. 12). If an elliptical bloom area is simulated, $a(t)$ is identical to $r_p(t)$, while a constant a/b ratio is kept.

The bloom area spreads in time. We assume a constant dilution time scale τ = 10 d, which characterizes the spreading of the fertilised patch during EisenEx and other iron-fertilisation experiments (Boyd et al. 2007). Patch spreading is given by an increasing patch radius:

$$r_p(t) = r_{p0}\sqrt{e^{t/\tau}} \quad (12)$$

Vertical decline of surface diatom carbon concentration is determined by f_v, defined as:

$$f_v = 0.5 - 0.5 \times \tanh[h_t^{-1}(z - z_{mt})] \quad (13)$$

The steepness of the concentration decline at the mixed layer base is regulated by the slope factor h_t, which is set to a constant value of h_t = 15 m in all simulations.

Substantial numbers of diatoms were observed below the mixed layer during EisenEx and EIFEX, without temporal trend or differences between the fertilised and non-fertilised area. Diatom carbon concentration found at 150 m amounted to 8–24% of surface concentration outside and 1–5% at the highest diatom concentration inside the bloom area during EisenEx (Assmy et al. 2007).

To fit the observed field distribution, we add a share which is constant in time, C_{sub}, to the variable share of the diatom distribution (Eq. 10). C_{sub} defines a profile with zero concentration in the upper layer and sharp concentration increase towards the bottom of the mixed layer. The concentration reaches a maximum below the mixed layer and declines linearly beneath with increasing depth. For simplicity, we assume a constant concentration reached at 160 m (vertical extent of the model domain) in all simulations, which is chosen to match the field distribution during EisenEx (Fig. 1a). It is equivalent to a percentage of 18 and 3% relative to the surface concentration outside and the highest diatom carbon concentration inside the bloom area, respectively.

$$C_{sub} = 0.45 \times \left(1 - 0.7 \times \frac{z - z_{mt}}{z_{max} - z_{mt}}\right) \times \{0.5 + 0.5 \tanh[h_t^{-1}(z - z_{mt})]\} \quad (14)$$

Initialisation

The development of a diatom patch is initiated after a spin up time of 7 model days. During this time a steady state vertical distribution of *Oithona* spp. individuals is reached under the low diatom 'outpatch' condition (see 'Flow field and model geometry'). After initialisation the simulation spans a period of 21 d, corresponding to the duration of the iron fertilization experiment EisenEx. A definition of the model parameters and range of values used are listed in Table 1.

RESULTS

The stochastic and directional motion of copepod individuals modifies the overall vertical copepod distribution in time. Distributional changes are represented in the following in terms of the development of the correlation coefficient between diatom carbon and copepod depth distribution. This vertical correlation is denoted by c_v, the horizontal correlation of copepod

and diatom carbon distribution by c_h. If not otherwise stated, c_v refers to the vertical correlation at the patch centre (r ≤ 1000 m) followed by a parenthesised c_v value referring to the entire inpatch area.

The horizontal distribution of copepods is given in terms of a relative abundance that refers to the initial abundance per unit area. The characteristic relative abundance within the outpatch area thus is 1. Changes in copepod abundance within a certain depth interval are referenced to the corresponding mean outpatch abundance and are given as percent change.

Uncertainty in the determination of the actual depth distribution in the field (see 'Discussion') requires consideration of a characteristic range of vertical steady state distributions outside and migratory responses of *Oithona* spp. inside the bloom area, forced by varying attraction (α) and repulsion weights (β, γ). This range is characterized by a relatively stable increase in abundance at the patch centre (see 'Model sensitivity').

Reference run

In terms of the diatom attraction weight (α) and repulsion coefficient (β), the range of values at which a moderately varying abundance increase is observed is centred at α = 4 and β = 2, if the surface avoidance weight is γ = 1.5. These settings are used for a reference simulation, by which a strong directional response along the diatom gradient is forced and a pronounced directionality of copepod motion due to repulsion by other individuals. Swimming speed of copepods is assumed to be V_A = 1 mm s^{-1}.

The vertical extent of the food rich layer (z_{mt} = 70 m) and the flow field are given with regard to the situation during the iron fertilisation experiment EisenEx. Inertial oscillations with an amplitude V_H = 0.2 m s^{-1} are superimposed on the geostrophic flow field.

Using this set of parameters the vertical correlation between copepods and diatom carbon (c_v) increases asymptotically to 0.83 at the patch centre and 0.77 within the entire inpatch area, respectively, which is close to the lower limit of c_v derived from observations during EisenEx (Fig. 2). After the initialisation period a constant c_v value of 0.67 is reached in the outpatch area. This value represents the upper limit of c_v within the low-food environment during EisenEx (Fig. 2).

During the initialisation period, the homogenous initial copepod distribution changes towards a pattern with a higher number of animals within the diatom enriched layer until a steady state distribution is reached (Fig. 3a). In the patch there is a continuous copepod immigration into the diatom-rich layer, which is supplied by an inward drift of animals from surroundings in deeper layers and their subsequent upward vertical migration (Fig. 3b). Supply of deep-dwelling individuals counters the depletion of *Oithona* spp. stock below the mixed layer in the patch area. Its decrease is moderate and exceeds a percentage decrease of 50% relative to the abundance outside the patch only towards the end of the experiment. In contrast, the number of *Oithona* spp. individuals at the patch centre (radius, r ≤ 1000 m) gradually increases by 150% in the mixed layer and by 70% in total (160 m) relative to the outpatch abundance.

The horizontal copepod and diatom distribution is highly correlated after Day 5 in the fertilised area (c_h > 0.9, progression not shown here). Significant abundance increase of *Oithona* spp. in the diatom-rich surface layer (>15%) is limited to an area enclosed by a radius of about 0.6 r_p around the patch centre at Day 21. Consequently, net abundance increase (0 to 160 m) is limited to the inner part of the patch area where the increase in diatom carbon concentration exceeds approximately 20% of its increment at the patch centre (Fig. 4a,b).

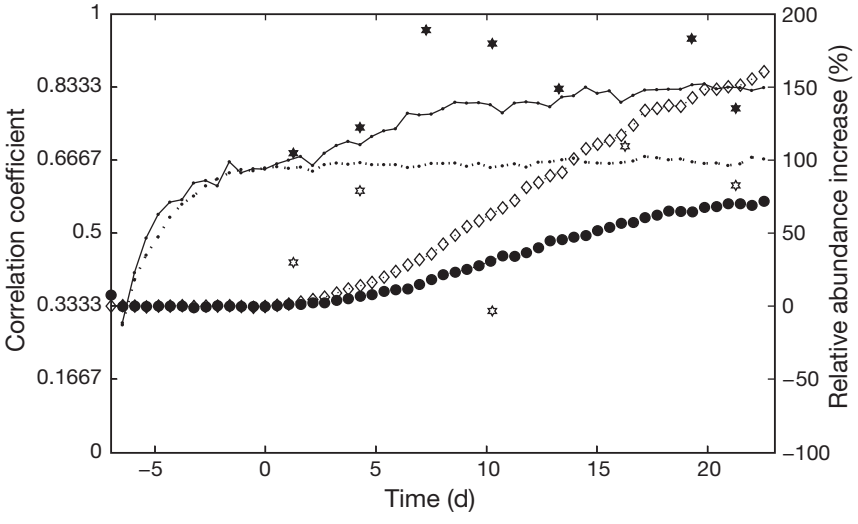

Fig. 2. *Oithona* spp. Modelled temporal development of relative copepod abundance at the patch centre, given as percent increase relative to outpatch abundance within the mixed layer (◇) and over 160 m (●). Lines represent the temporal development of the correlation coefficient between vertical copepod and food distribution (in terms of diatom carbon concentration) in the outpatch area (·····) and at the patch centre (–·–·–). The development of vertical correlation during EisenEx iron fertilization experiment (field situation) is given by open (outpatch) and filled (inpatch) stars (3 d mean)

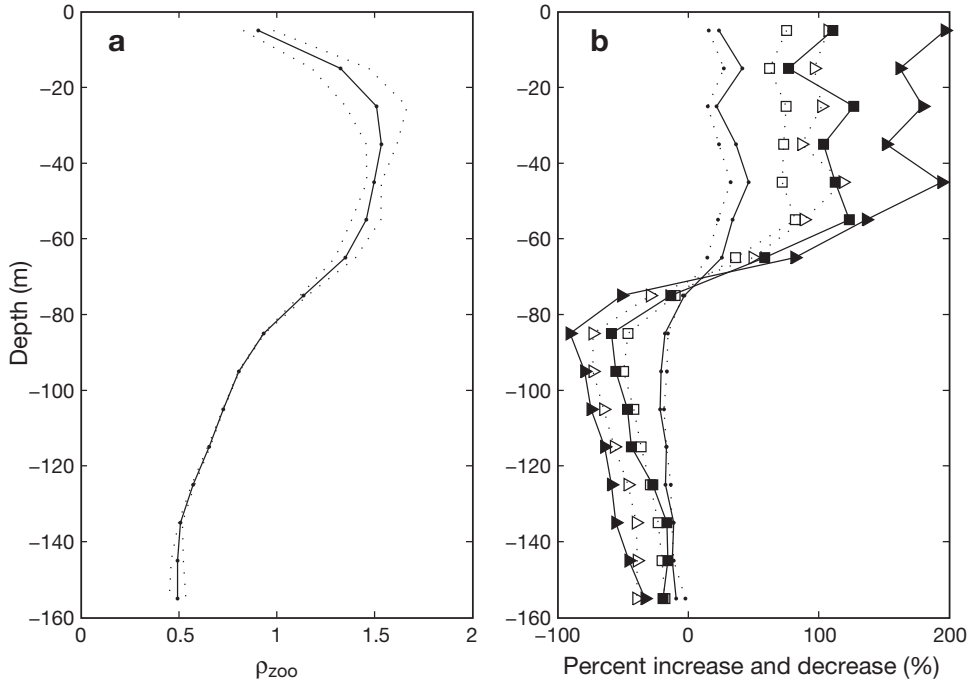

Fig. 3. *Oithona* spp. (a) Mean vertical distribution of copepods in the outpatch area after the initialisation period during the reference run (solid line). Dotted lines represent 1 SD. ρ_{zoo}: local copepod density. (b) Relative depth-dependent copepod abundance increase and decrease at the patch centre (solid lines, filled markers; r ≤ 1000 m) and central inpatch area ($<r_p/2$, where r_p is patch radius) (dotted lines) at Days 7 (dots), 14 (squares) and 21 (triangles) relative to the vertical outpatch distribution

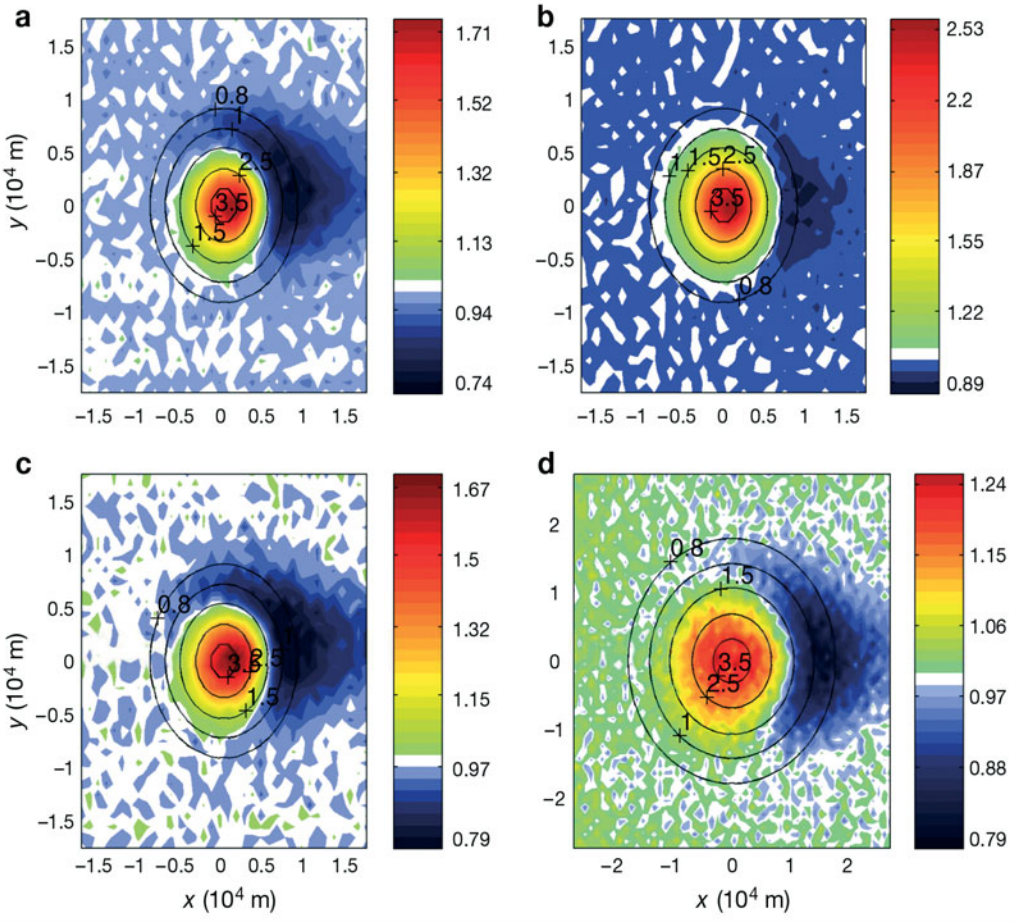

Fig. 4. *Oithona* spp. Horizontal copepod distribution at Day 21 after fertilisation during the reference run, given in terms of the relative copepod increase within (a) the total water column (160 m) and (b) the mixed layer referenced to the outpatch (steady state distribution). Surface diatom carbon concentration (µmol C l^{-1}) is indicated by isolines. (c) Horizontal copepod distribution at Day 21 (160 m) within the EIFEX flow field, using otherwise unchanged model settings. (d) Resulting distribution using the EIFEX flow, a mixed layer depth of 120 m, and a doubled patch radius

Sensitivity study

Effects of varying α, β and γ

For the sensitivity study the weights α, β and γ have been changed in the range of 0.5 to 8, 0 to 4 and 1 to 2, respectively, while keeping all other parameters constant and equal to their standard values (Table 2). With the increasing diatom attraction coefficient (α) the vertical steady state outpatch distribution of *Oithona* spp. shows a progressively increased abundance within the upper layer and depletion below (Fig. 5a). In the patch, copepod abundance within the diatom rich layer steeply increases with the increasing diatom attraction coefficient (α) by a maximum of 150% at an α value of 4 (Fig. 5b). With further increase in α, the relative abundance increase is lower, i.e. 90%, at an α of 8, corresponding to a α:β ratio of 4 (Fig. 5b).

With the increasing repulsion coefficient (β) the vertical steady state outpatch distribution of *Oithona* spp. shows a progressively declining number of individuals within the mixed layer and changes to a homogenous vertical distribution (Fig. 5c). Inpatch abundance within the diatom-rich layer increases by 50% at a β of 0.5 (α:β = 8) and shows a maximal increase of 150% at a α:β ratio of 2 (Fig. 5d). With a further increment of β the abundance increase is gradually weakened to 110% at a β of 4, corresponding to a α:β ratio of 1 (Fig. 5d).

The progression of the net abundance increase (0 to 160 m) is dampened in relation to the increase within the mixed layer. Within a range of α and β weights, corresponding to a α:β ratio of 1 to 4, the total abundance increase varies from 50 to 70%. The abundance below the mixed layer is reduced by 30% relative to the outpatch abundance at a α:β ratio of 1, however,

Table 2. Model results. *a*/*b* ratio of semi-major and semi-minor axes, given the food patch extent and shape at Day 21. EE: EisenEx; EF: EIFEX; NOG: no geostrophic flow. c_{vin}: vertical correlation of copepods and diatom carbon (c_v) at Day 21 in total inpatch area; c_{vinC}: c_v at the patch centre (radius, r < 1000 m); c_{vout}: c_v in the outpatch; and c_h: horizontal correlation of copepods and diatom carbon at Day 21. See also Table 1 for parameter definitions. Copepod increase is given in terms of increase relative to the outpatch abundance (steady state distribution) in total and within the mixed layer, which, for example, is 1.7- and 2.52-fold, respectively, in the reference run (**in bold**)

α	β	γ	z_{mt}	V_A	V_H	Flow field	*a*/*b* Day 21 (10^4 m)	c_{vin}	c_{vinC}	c_{vout}	c_h	Copepod increase (160 m)	Copepod increase (z_{mt})
4	**2**	**1.5**	**70**	**0.001**	**0.2**	**EE**	**1/1**	**0.77**	**0.84**	**0.66**	**0.92**	**1.70**	**2.52**
4	2	1.5	70	0.001	0	EE	1/1	0.73	0.80	0.67	0.82	1.45	2.17
0.5	2	1.5	70	0.001	0.2	EE	1/1	0.18	0.43	0.04	0.82	1.11	1.38
1	2	1.5	70	0.001	0.2	EE	1/1	0.41	0.64	0.19	0.87	1.25	1.72
2	2	1.5	70	0.001	0.2	EE	1/1	0.63	0.75	0.4	0.9	1.46	2.19
3	2	1.5	70	0.001	0.2	EE	1/1	0.73	0.83	0.57	0.91	1.61	2.45
6	2	1.5	70	0.001	0.2	EE	1/1	0.78	0.85	0.76	0.93	1.72	2.34
8	2	1.5	70	0.001	0.2	EE	1/1	0.74	0.79	0.78	0.92	1.55	1.91
4	0.5	1.5	70	0.001	0.2	EE	1/1	0.70	0.79	0.83	0.85	1.40	1.50
4	0.75	1.5	70	0.001	0.2	EE	1/1	0.75	0.78	0.85	0.9	1.55	1.80
4	1	1.5	70	0.001	0.2	EE	1/1	0.79	0.81	0.84	0.91	1.65	2.08
4	1.5	1.5	70	0.001	0.2	EE	1/1	0.78	0.80	0.78	0.92	1.69	2.38
4	3	1.5	70	0.001	0.2	EE	1/1	0.68	0.78	0.48	0.91	1.56	2.37
4	4	1.5	70	0.001	0.2	EE	1/1	0.60	0.75	0.38	0.91	1.41	2.10
4	2	1	70	0.001	0.2	EE	1/1	0.77	0.87	0.69	0.92	1.70	2.54
4	2	2	70	0.001	0.2	EE	1/1	0.76	0.80	0.65	0.92	1.69	2.51
4	2	1.5	20	0.001	0.2	EE	1/1	0.60	0.73	0.36	0.87	1.38	3.49
4	2	1.5	30	0.001	0.2	EE	1/1	0.68	0.73	0.46	0.90	1.49	3.25
4	2	1.5	40	0.001	0.2	EE	1/1	0.73	0.78	0.55	0.91	1.64	3.22
4	2	1.5	50	0.001	0.2	EE	1/1	0.75	0.78	0.61	0.91	1.70	3.02
4	2	1.5	90	0.001	0.2	EE	1/1	0.72	0.82	0.71	0.90	1.49	1.92
4	2	1.5	120	0.001	0.2	EE	1/1	0.62	0.77	0.76	0.88	1.30	1.44
4	2	1.5	70	0.001	0.2	EF	1/1	0.75	0.80	0.67	0.93	1.65	2.45
4	2	1.5	70	0.000	0.2	EE	1/1	0.79	0.87	0.71	0.90	1.59	2.3
4	2	1.5	70	0.001	0.2	NOG	1/1	0.75	0.83	0.67	0.86	1.52	2.4
4	2	1.5	70	0.001	0.2	EE	2/2	0.73	0.81	0.66	0.75	1.46	2.22
4	2	1.5	70	0.001	0.2	EE	2/1	0.75	0.82	0.66	0.84	1.59	2.42
4	2	1.5	70	0.001	0.2	NOG	2/2	0.7	0.82	0.66	0.68	1.22	1.95
6	2	1.5	70	0.001	0.2	EE	2/1	0.75	0.79	0.76	0.86	1.57	2.15
4	2	1.5	120	0.001	0	EF	2/2	0.59	0.76	0.75	0.78	1.21	1.35

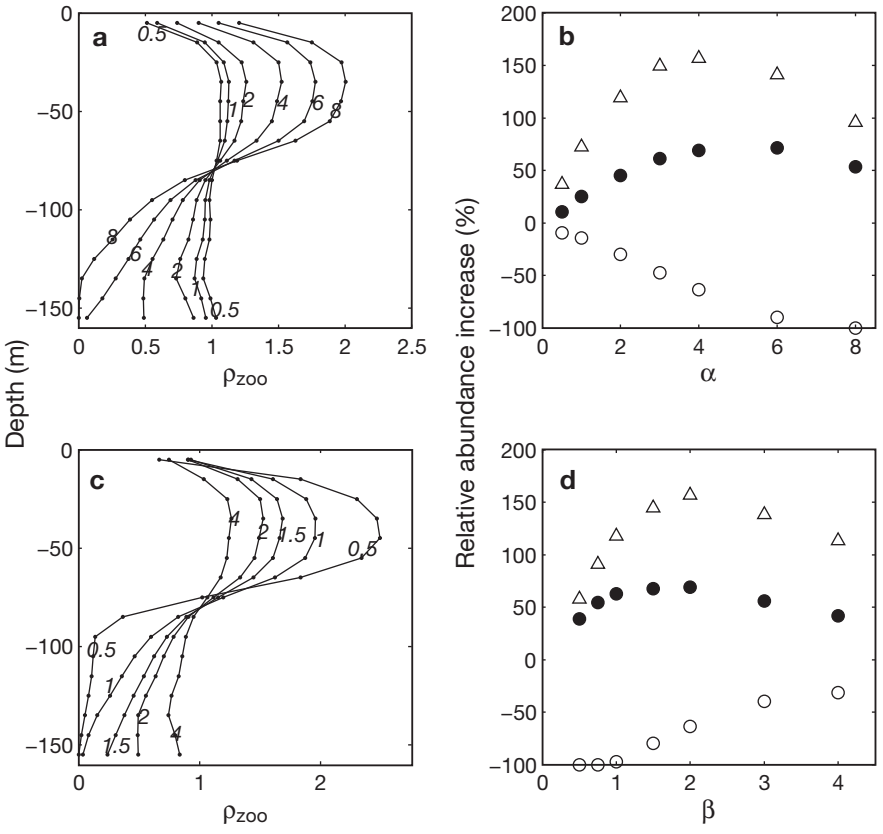

Fig. 5. *Oithona* spp. Sensitivity study: (a) mean vertical animal distribution (steady state) outside the patch dependent on the food attraction coefficient (α). Single profiles are marked by the respective α-value (numbers in italics). ρ_{zoo}: local copepod density. (b) Relative abundance increase at the patch centre at Day 21 in the mixed layer (△), below the mixed layer (○) and over 160 m (●), relative to the respective outpatch abundance and plotted against α. (c,d) Analogous plots for the varying repulsion coefficient (β)

declines within this range to a nearly complete exhaustion with an increasing α:β ratio. (Fig. 5b,d).

Changing the surface avoidance coefficient (γ) within a range of 1 to 2 has a minor effect on the model outcome. The vertical correlation between food and copepod distribution declines at the patch centre from c_v = 0.87 to 0.80 and outside the patch from c_v = 0.69 to 0.65 with increasing γ (Table 2). Abundance increase at the patch centre does not change significantly within the mixed layer and in total (0 to 160 m), respectively (Table 2).

Effects of varying mixed layer depth

The effect of different mixed layer depths was explored within the z_{mt} range of 20 to 120 m, which affects the vertical diatom distribution (see 'Diatom distribution') and the profile of inertial motion (Eq. 8) in the model. Other settings were retained unchanged with respect to the reference simulation.

The steady state distribution of *Oithona* spp. which develops outside the patch is changed with changing depth of the mixed layer. Mean ρ_{zoo} within the mixed layer increases from 1.25 to 1.4 when z_{mt} changes from 20 to 50 m, and decreases again with increasing z_{mt} ca. 1.2 for a depth of 120 m (Fig. 6a). Mean ρ_{zoo} below the mixed layer decreases nearly linearly from 0.95 to 0.45 within the z_{mt} range from 20 to 120 m (Fig. 6a).

The percentage increase in copepod abundance which is observed within the mixed layer at the patch centre relative to the respective outpatch abundance is reduced nearly linearly with increasing z_{mt} (Fig. 6b, triangles). Maximum percentage increase is 250% within the shallowest mixed layer (20 m). The minimum percentage increase is 50%, reached within the deepest mixed layer (120 m).

The net abundance increase (0 to 160 m) rises to a maximum increase of about 70% for z_{mt} in the range 40 to 80 m (Fig. 6b, filled circles). Within this range the abundance below the mixed layer declines nearly linearly with increasing z_{mt}, and shows a percentage decrease relative to the respective outpatch abundance of 20% for a z_{mt} of 40 m and more than 70% for a z_{mt} of 80 m (Fig. 6b, open circles).

The correlation coefficient of the vertical diatom carbon and animal distribution, c_v, follows the progression of net abundance increase within the bloom area. It increases to 0.75 and subsequently declines again to 0.6. Within the outpatch area c_v increases asymptotically to 0.76 with deepening mixed layer depth (Table 2). The horizontal correlation coefficient of diatom carbon and copepod distribution (c_h) is only

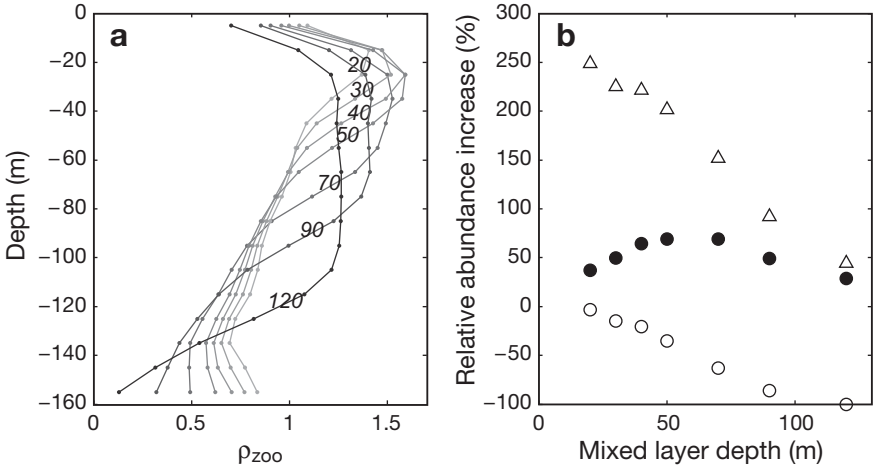

Fig. 6. *Oithona* spp. Sensitivity study: (a) mean vertical animal distribution (steady state) outside the patch dependent on mixed layer depth (20, 30, 40, 50, 70, 90, 120 m, numbers in italics). (b) Relative copepod abundance increase in the patch centre at Day 21 in the mixed layer (△), below the mixed layer (○) and over 160 m (●) dependent on the mixed layer depth, relative to the respective outpatch abundance. Except depth of mixed layer, settings remained unchanged with respect to the reference run

weakly affected by different mixed layer depths and varies in the range from 0.87 to 0.91 at Day 21 (Table 2).

Effects of copepod swimming speed

Along with a lower swimming speed, V_A, deep-dwelling animals have a reduced probability of entering the shallower transition zone between food-depleted and food-enriched layers, where upward migration is forced along a steep diatom gradient.

Using a swimming speed of 0.5 mm s^{-1} (as compared to 1 mm s^{-1} in the reference run), c_v increases to 0.87 in the patch centre and 0.79 within the entire food patch area, respectively, and is 0.71 outside the patch (Table 2). The horizontal copepod and diatom carbon distribution is highly correlated ($c_h > 0.9$) after Day 7, which is slightly delayed with respect to the reference run. The abundance increase of *Oithona* spp. is weakened to a percentage increase of 130 and 60% relative to the outpatch abundance within the mixed layer and in total (0 to 160 m), respectively (Table 2).

Effects of different flow fields

To explore the impact of inertial oscillation, this flow component is simulated without stationary flow ($u_s(z) = 0$). The correlation between vertical copepod and diatom carbon distribution, c_v, approaches a value of 0.83 in the patch centre and 0.75 in the total bloom area after 2 wk; c_v is 0.67 in the outpatch area (Table 2). The horizontal distribution of copepods and diatom carbon is highly correlated and peaked at 0.94 at Day 6, but gradually decreases to 0.85 at Day 21 (Table 2). Percentage increase in copepod abundance at the patch centre is 140% within the diatom-rich layer relative to the outpatch abundance. Net abundance increased by 50% (0 to 160 m) until Day 16 (Table 2).

Inertial oscillation causes a wobbling of the surface layer. The resultant circular displacement of the diatom patch changes the local vertical gradients of diatom concentration and copepod abundance inside the bloom area and in its periphery. The actual migration behaviour of a deep-dwelling individual is subject to the steepness of these gradients (Fig. 7a). Upward migration is increasingly forced with increasing surface diatom concentration when diatom attraction outweighs the repulsive effects of other individuals. This dependency causes a net displacement of copepods along the horizontal diatom gradient towards the centre of the bloom area (Fig. 7b). Net abundance increase within the bloom area is gained from the surroundings and depends on the ratio of the area affected by the wobbling diatom patch to the diatom patch area itself, A_i. Regarding a circular food patch, A_i is given by:

$$A_i = \frac{(r_p + r_i)^2}{r_p^2} \quad (15)$$

as a function of the food patch radius, r_p, and radius of inertial oscillation, r_i. In the simulations r_i is ca. 1850 m and the area ratio is about 1.5, 1.3 and 1.2 for patch areas of 300, 600 and 1200 km^2, respectively.

Inertial oscillation which is superimposed on a stationary flow field contributes significantly to the abundance increase inside the bloom area and causes deflection of the paths of copepod individuals towards the patch centre line (Fig. 7c).

Simulating the EisenEx flow field without inertial oscillation, c_v increases to 0.81 at Day 11 at the patch centre and to 0.73 in the total bloom area; c_v is about 0.67 outside the patch. The increase in c_h is weakened and flattened in comparison to the reference simulation with inertial oscillation. It approaches 0.82 at

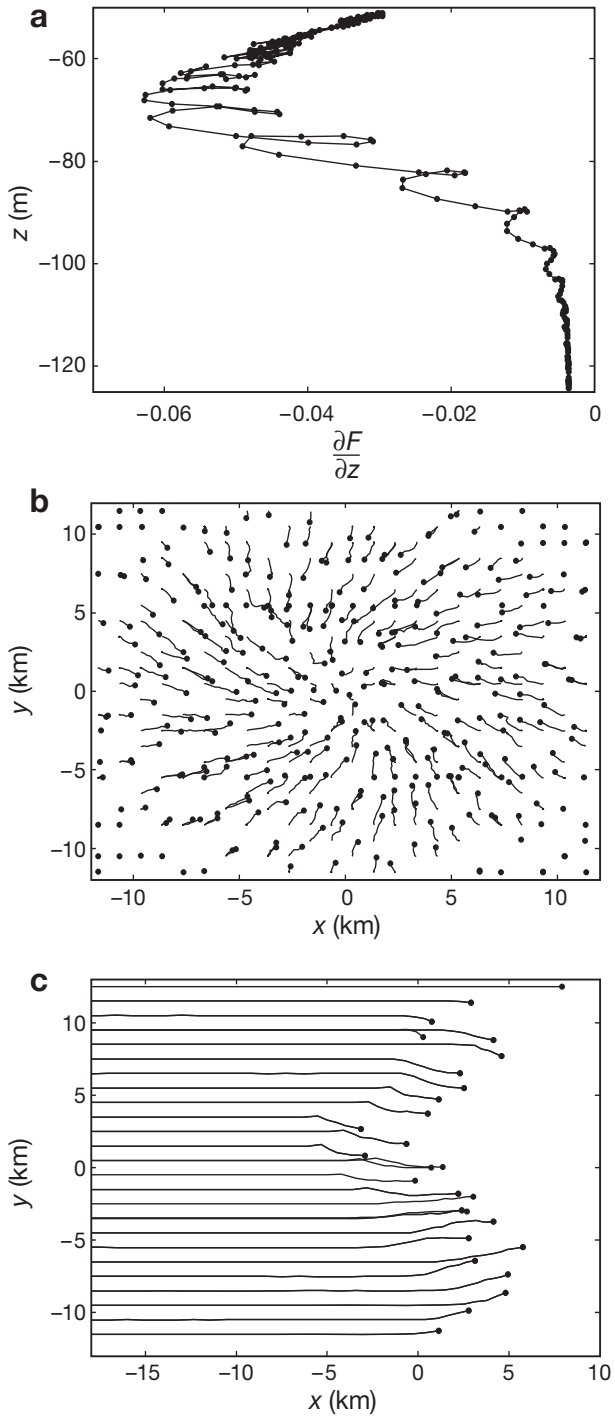

Fig. 7. *Oithona* spp. (a) Ascent of a copepod individual triggered by the steepness of the food gradient. *F*: food density (diatom carbon concentration); *z*: depth. (b) Net horizontal displacement of individuals that show such migratory behaviour in a flow field governed by inertial oscillation, illustrated by the path of different individuals (short line) and their final horizontal position (black dots). (c) Paths of ascending copepods in a flow field that is governed by geostrophic flow and inertial oscillation. Their paths show a deflection along the horizontal food gradient. Paths in (b) and (c) are given as an average position over one period of inertial oscillation

ca. Day 11 after fertilisation. *Oithona* spp. abundance increases at the patch centre by 115 and 40% within the mixed layer and over 160 m, respectively, compared to an increase by 150 and 70% with superimposed inertial oscillations (Table 2).

In a further simulation, we investigate the effects caused by the differences in the stationary EisenEx and EIFEX flow fields. In the simulation considering the EIFEX flow field with superimposed inertial oscillations, c_v increases to 0.8 and 0.75 at the patch centre and in the total bloom area, respectively, and is about 0.67 in the outpatch area. The horizontal correlation between copepod and diatom carbon distribution approaches 0.93 at ca. Day 8 after fertilisation. *Oithona* spp. abundance in the centre of the bloom area increases by 145% within the mixed layer and shows net increase (160 m) by 65% (Fig. 4c), which is slightly less than the respective increases in the EisenEx flow field.

Effects of diatom patch extent

To explore the impact of the diatom patch dimension and shape, firstly r_p is doubled compared to the reference run; the surface area thus is increased by a factor of 4. The patch radius increases to 20 km at Day 21 in the respective model runs. Within the EisenEx flow field and retaining other parameters unchanged with respect to the reference simulation, c_v is slightly reduced and increases to 0.81 at the centre and 0.73 within the total bloom area (Table 2). The horizontal correlation of diatom and copepod distribution varies periodically with inertial oscillations and peaks at Day 11 with a c_h of 0.8 (±0.015) and gradually decreases thereafter to 0.75 at Day 21. The relative copepod abundance at the patch centre increases by 120 and 45% within the mixed layer and over 160 m, respectively (Table 2). Like the results of the reference run, net abundance increase is limited to the inner part of the patch area where the increase in diatom concentration exceeds approximately 20% of its increment at the patch centre. However, there is a strong depletion of animals inside the food patch upstream at a distance $>r_p/2$. The doubling of the patch radius leads to a reduced increase in copepod abundance at the patch centre, which is equivalent to 88 and 86% of the increase during the reference simulation within the mixed layer and over 160 m, respectively.

Prescribing an elliptical shape for the diatom patch (semi-major axis (*a*)/semi-minor axis (*b*) = 0.5, *a* = 20 km at Day 21) and aligning the semi-major axis (*a*) in the direction of the stationary flow, c_v increases to about 0.82 at the centre and 0.75 within the total bloom area (Table 2). The horizontal correlation is maximal at

Day 12 (c_h = 0.88) and declines thereafter to 0.84 (Day 21) while it varies periodically. The copepod abundance at the patch centre is raised by 140 and 60% within the mixed layer and over 160 m, respectively, equivalent to an increase of about 96 and 94%, respectively, relative to the increase in the reference run (Table 2).

EIFEX experiment

In order to approximate the field situation during EIFEX, a mixed layer depth of 120 m and a final patch radius of 20 km (Day 21) is simulated. During the model run c_v is 0.75 outside the patch, c_v increases to 0.8 at Day 10 at the centre of the bloom area but declines again to 0.76 at Day 21. Within the total bloom area it decreases continuously to 0.59. Horizontal correlation between diatom carbon concentration and *Oithona* spp. abundance, c_h, increases to 0.82 at Day 14 and decline thereafter to 0.78 (Day 21) while varying periodically with inertial oscillations. The copepod abundance at the patch centre shows a percentage increase of 35% relative to the outpatch abundance within the mixed layer and a net increase of 20% (160 m, Fig. 4d).

DISCUSSION

In this simulation study, we have explored the magnitude of changes in horizontal copepod distribution which are caused by directional vertical migration in a bloom area in the vertical sheared flow fields at the sites of the iron fertilisation experiments EisenEx and EIFEX.

EisenEx field findings and simulation results

During EisenEx, *Oithona* spp. was sampled at the discrete depths of 10, 20, 40, 60, 80, 100 and 150 m at 5 outpatch and 13 inpatch stations with a Niskin bottle with a sampling volume of 12 l. Estimates of the abundance in different depth strata are based on trapezoidal integration of the estimates at the discrete sampling depths (Henjes et al. 2007). The mean outpatch abundance of *Oithona* spp. copepodites and adults was 9 ind. l^{-1} (0 to 150 m), which corresponds to ρ_{zoo} = 1 in the simulation study.

The vertical distribution of *Oithona* spp. was centred below or near the bottom of the mixed layer outside the fertilised area. The depth-integrated abundance over the depth range 60 to 150 m and 80 to 150 m, respectively, amounted to 60% (30 to 95%) and 30% (20 to 55%) on average of the integrated abundance in the upper 60 m of the water column. The relative amount of deep-dwelling copepods (60 to 150 m) was 75% on average without the first outpatch station with a comparable shallow *Oithona* spp. distribution.

The integrated abundances equate to a mean outpatch concentration of ca. 13.5 ind. l^{-1} in the upper 60 m. Generally, the single abundance estimates showed large variability. Sampled abundance varied in the range of 3 to 25, 3 to 25, 1.8 to 7.2 and 0 to 5.6 ind. l^{-1} at 60, 80, 100 and 150 m outside the patch, while the mean abundance was 15, 11, 3.8 and 1.7 ind. l^{-1}, respectively (Fig. 8).

The simulated vertical outpatch distribution corresponds approximately to the mean abundances sampled at different depths during EisenEx if a food attraction coefficient α = 6 and a repulsion coefficient β = 2 is used (Fig. 8). However, in view of the mean vertical distribution without the first outpatch station, this

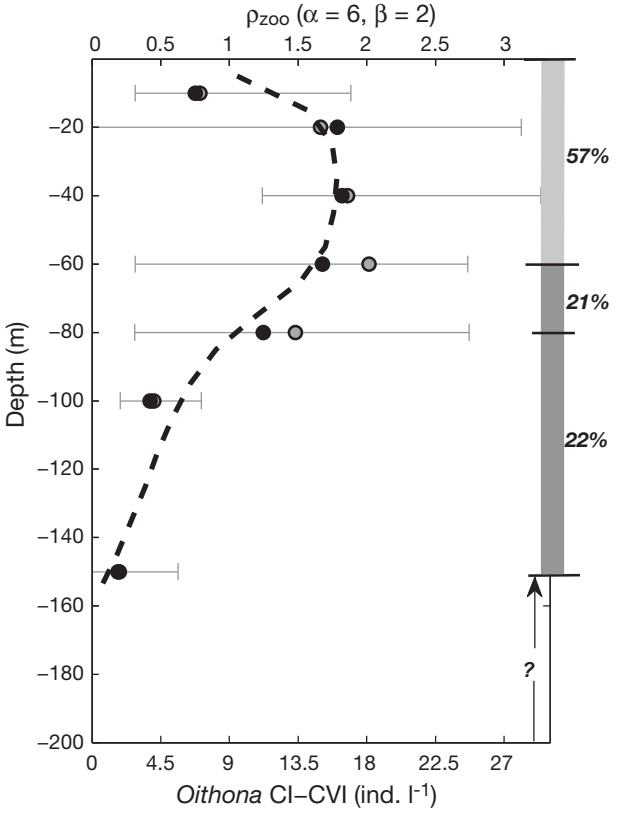

Fig. 8. *Oithona* spp. Mean abundance of *Oithona* spp. sampled at different depths during EisenEx outside the phytoplankton patch including (●) and excluding (◍) the first oupatch station. Simulated mean vertical distributions are shown by the black dashed line for the food attraction coefficient α = 6 and repulsion coefficient β = 2. Gray horizontal bars indicate the minimum and maximum abundances of *Oithona* spp. sampled at the discrete sampling depth. Percentage of *Oithona* spp. individuals found on average at outpatch stations (excluding the first station) in the upper 0–60, 60–80, 80–150 m of the total individuals in upper 0–150 m is given on the right hand side of the graph

simulated vertical distribution may underestimate the proportion of individuals which reside near below the surface layer.

Compared to EisenEx, large number of *Oithona* spp. individuals were sampled during EIFEX at 150 m (11 ind. l^{-1} on average) and even at depths of 200 and 250 m (see 'EIFEX experiment' below). This large number of markedly deep-dwelling individuals could imply that the sparse vertical resolution and the very small sampling volume had caused an underestimate of the number of *Oithona* individuals below 100 m during EisenEx. Consequently, in the simulation study we account for a range of vertical *Oithona* spp. distributions outside the patch.

Whether very deep-dwelling *Oithona* spp. (>150 m) respond with upward migration below a phytoplankton bloom or whether they occasionally re-enter the upper 150 m of the water column is unknown and not covered by the simulation study.

At the patch centre, *Oithona* spp. individuals migrated into the phytoplankton-rich surface layer. A transient downward displacement of individuals occurred after 2 storm events (at the end of the first and the second week of EisenEx). The strong decrease in abundance below the mixed layer at the patch centre which is shown in simulations (e.g. $\alpha = 6$, $\beta = 2$) was only observed at single stations.

The number of *Oithona* spp. individuals at patch centre increased by up to 15 ind. l^{-1} in the upper 60 m of the water column over the course of EisenEx. This increase is 1.5 times the integrated outpatch abundance (m^{-2}) in the deeper layer between 60–150 m and 3 times the integrated abundance over the depth range 80–150 m. Sampling suggests net increase of up to 7 ind. l^{-1} (0 to 150 m), which would correspond to an increase by 80% of the mean outpatch abundance, but maybe is not properly assessed due to the low vertical resolution.

Oithona spp. were only sampled near or at the centre of the phytoplankton patch. Sampling thus gives no information about the horizontal distribution pattern of *Oithona* spp. within the fertilised area.

The simulation results show a quite stable net increase in *Oithona* spp. abundance at the patch centre of approximately 70% of the outpatch abundance in the α:β ratio range of 2 to 3 (Fig. 5b,c). Simulation results with an elliptical shaped patch approximating the field situation during EisenEx show a slightly lower abundance increase compared to the standard patch simulation (Table 2). In both cases a significant abundance increase is limited to the central patch area and show a maximal increase at the patch centre. In the simulation with $\alpha = 6$ and $\beta = 2$ ($a/b = 0.5$; Table 2), the net abundance increase is ca. 60% at the patch centre and 25% on average in the area where the surface diatom carbon concentration have a more than 2-fold increase relative to the outpatch (180 km^2). The respective abundance increases are ca. 110 and 60% in the mixed layer.

Effects of the model simplifications

In the field, storm events forced deepening of the mixed layer depth over the course of EisenEx from 30–40 m at the very beginning of the experiment to 80–90 m at the end (Cisewski et al. 2005). The depth distribution of the diatoms observed during EisenEx would correspond to a vertical diatom distribution in a simulation with variable z_{mt}, increasing from ca. 60 to 80 m. In the simulation, shallowing (60 m) or deepening (80 m) of z_{mt} shows converse effects on the abundance increase within the mixed layer and abundance decrease below (Fig. 6), and a constant mixed layer depth (z_{mt} = 70 m) is assumed as a standard in the simulation study for simplicity.

A circular diatom patch which increases in extent to a final diameter of 20 km (Day 21) is used as standard in the simulation study. The diatom patch had a variable, elongated shape during EisenEx, with a larger patch extent aligned to the stationary flow (Bakker et al. 2005). Shape and area increase in the diatom patch may be well approximated by an elliptically shaped patch that increases in extent to a final length of 40 km and final width of 20 km (τ = 10 d; $a/b = 0.5$; a = 20 km at Day 21).

Simulation results show a minor effect of an increased patch length on the abundance increase in the bloom area (see 'Effects of diatom patch extent'). Net abundance increase at the patch centre and abundance increase within the mixed layer amounted to 94 and 96% of the respective increments during the reference run with a standard patch.

The small impact of an increased patch length is due to the effects of inertial motion, which gives rise to a net displacement of animals towards the patch centre (see 'Effects of different flow fields'). This net displacement of *Oithona* spp. individuals within the patch and from the surroundings can take place along smallest patch dimension (semi-minor axis), because of the circular relative motion of deep-dwelling copepods and the surface layer.

Inertial motion is caused by transient wind events which set water in motion, which continues to move in a circular trajectory subject to the Coriolis force. Rapid changes of strong winds produce the largest oscillations. During EisenEx, inertial motion was forced by a sequence of strong wind events and showed periods of intensification and decay and furthermore showed vertical variability. In the model, we define an idealised inertial motion and assume a characteristic, constant amplitude, V_H, and an invariable vertical extent (constant z_{mt}).

The simulated flow field is a major simplification of the actual flow field at the experimental site, which in reality gives rise to more complex patterns of copepod redistribution. The model simplification, however, may lead to a substantial underestimate of the area which was covered by the relative displacement of the phytoplankton patch and subsurface layer and thus of the number of copepods which can enter the food-rich surface layer from below.

Uncertainties in field data and interpretation

In view of the number of small copepods sampled at 100 and 150 m, Henjes et al. (2007) conclude that their abundance increase in the phytoplankton bloom area could not be explained by upward migration alone. Differences in the conclusions drawn by Henjes et al. (2007) and by the present study are partly due to a different interpretation of the field abundance data, which shows high variability but was sampled with low resolution. Furthermore, Henjes et al. (2007) assume a high abundance increase similar to that observed at the patch centre for a wide extent of the fertilised area, while the simulation study shows a maximum increase at the patch centre and an abundance gradient within the patch. The different assessment, however, is also due to a different estimate of the area swept over by the patch and of the depth range in which substantial inflow of *Oithona* spp. individuals occurs below the patch.

The simulation study shows that especially the displacement of the surface layer relative to the deeper layer, which is caused by surface currents (e.g. inertial oscillations), allows for a large abundance increase which explains most of the estimated increase during EisenEx. Thus, besides inflow of individuals well below the mixed layer (e.g. >100 m) whose drift is mainly determined by the stationary flow field, the accumulation of *Oithona* spp. in a bloom area should critically depend on the number of those deep-dwelling copepods which reside in proximity to the base of the mixed layer.

In view of the flow field simplification in the model and the possible underestimate of the number of markedly deep-dwelling *Oithona* spp. individuals during EisenEx, the simulation results should be considered as conservative estimates of the abundance increase that could have been caused by migratory response of *Oithona* spp. The much more complex displacement of the surface layer relative to the deeper layer in the real flow field may also partly explain why a strong decrease in *Oithona* spp. abundance below the phytoplankton-rich layer at the patch centre was only observed at single stations in the field. However, it has to be assumed that the low sampling resolution and the strong variability in abundance meant that it was not possible to resolve properly shifts in the abundance of *Oithona* spp. below the mixed layer.

The composition of the developmental stages of *Oithona* spp. indicates no advanced recruitment into copepodite stages inside the bloom area of EisenEx (Wend 2005). However, such growth signals could have been masked by the gradual accumulation of vertically immigrating copepods. Thus, higher recruitment rates may have added to the observed increase in abundance of *Oithona* spp. copepodites and adults during EisenEx.

EIFEX experiment

During EIFEX, a large number of *Oithona* spp. were sampled at 150 m and even at 200 and 250 m, showing mean abundances of 11, 7 and 6 ind. l^{-1}, respectively. About half of these individuals belonged to the species *Oithona similis*. No clear vertical and subsequent horizontal redistribution of *Oithona* spp. was observed during EIFEX (J. Henjes pers. comm.), which in part can be explained by the very deep vertical extent of the phytoplankton-enriched surface layer in accordance with the simulation results. However, we suppose that *Oithona* spp. was less attracted by the long-spined diatom species which dominated the EIFEX phytoplankton bloom.

Southern Ocean environment

Ward & Hirst (2007) found the abundance and fecundity rates of *Oithona similis* to be strongly related to temperature and depth-integrated chlorophyll *a* in the Southern Ocean, and found further indication of food limitation. These findings are in agreement with findings for other copepod species (e.g. Shreeve et al. 2002, Jansen et al. 2006).

Southern Ocean copepods have to cope with a strongly seasonal, patchy and overall dilute food environment. Most copepod species shift their diet towards an omnivorous feeding before and after the growth season, while diatoms dominate the diet in summer (Atkinson 1998, Pasternak & Schack-Schiel 2001). In the growth season, transient mesoscale phytoplankton blooms strongly increase the phytoplankton biomass locally and cause high horizontal patchiness of the food environment (Smetacek et al. 1990, Moore & Abbott 2002, Strass et al. 2002). Copepods have to face with periods of food shortage even in the growth season and need to utilise a wider range of food items to survive under the different conditions of food supply during their life span.

Oithona similis is known to feed on a variety of food items, including nauplii of other copepod species,

microzooplankton, fecal pellets, diatoms and other phytoplankton (Lampitt 1978, Hopkins 1985, Gonzales & Smetacek 1994, Atkinson 1998, Castellani et al. 2005). Ambush feeding behaviour and body construction bias the prey perception ability of *Oithona* spp. towards motile prey and larger immobile particles (Visser 2001), while a beneficial diet is restricted to food items which they are able to ingest with an effort that matches the particular nutritional gain.

Considerable difference in this respect even among diatoms of the same size class and biased perception ability may be reasons for conflicting reports on diet and feeding preference of *Oithona* spp. The rare dietary studies may be additionally biased by the investigation methods and by seasonal effects. They show diatoms as preferred food in the spring, summer and autumn (gut content analysis; Hopkins 1985, 1987, Hopkins & Torres 1989), a substantial amount of diatoms but preference for motile prey in the pre- bloom and post-bloom situation (gut content analysis and feeding experiments; Atkinson 1995, 1996), but also no confirmation of feeding on diatoms in the summer (fatty acid composition; Kattner et al. 2003).

Utilisation of a variety of food items likewise gives copepods the ability to prolong their residence periods in the deeper unproductive water column. It allows for the development of a food-finding strategy that includes deep-dwelling behaviour in areas with low surface phytoplankton concentration, which causes an increased drift out of areas with rare food in the surface layer. Thus, deep-dwelling would be a suitable mechanism for copepods to increase their chance of being advected from a low to a high food environment. Given the wide range of possible food for *Oithona* spp., the nutritional detriment during deep-dwelling periods should be moderate compared to the food gain due to an increased probability of being subsequently exposed to a food-rich environment.

In view of the vertical distribution of potential food items (e.g. Klaas 2001) the nutritional detriment should be especially small for deep-dwelling individuals that reside in proximity to the base of the mixed layer. Also these copepods are displaced great distances relative to the surface layer due to surface currents that cause not only wobbling but also non-circular displacement of the surface layer in the field. Whether *Oithona* spp. individuals that reside near below the mixed layer particularly benefit from their migration behaviour cannot be addressed with this simple model.

The strong migratory response of deep-dwelling copepods towards the progressively phytoplankton-enriched surface inside the bloom area during EisenEx is consistent with the food-finding strategy discussed above and provides a strong nutritional benefit for *Oithona* spp. individuals. In contrast, dominance of long-spined diatoms likely prevents an effective feeding on diatoms by *Oithona* spp. in the bloom area of EIFEX. The very deep extent of the phytoplankton-enriched layer and less attractive nature of the dominant diatom species may have caused the absence of a significant vertical and subsequent horizontal redistribution of *Oithona* spp. during this experiment.

CONCLUSION

An increase in copepod abundance was observed during 6 of 12 mesoscale iron fertilisation experiments. The experiments were conducted during different seasons and under different environmental abiotic conditions (such as temperature). During most of the experiments, which covered observation periods of 5 to 37 d, phytoplankton blooms were induced which were dominated by diatoms, but variable in species composition and abundance (Boyd et al. 2007).

A significant reproductive response may increase copepod abundance in warm environments which support short life cycles. This seems to have happened during IronEx II, conducted in the warm equatorial Pacific (Rollwagen Bollens & Landry 2000).

A lower mortality of copepod nauplii stages, caused by e.g. a diet shift of omnivorous predators in phytoplankton blooms, may lead to an increase in the number of copepodites relative to the outpatch. Such a mechanism is discussed by Tsuda et al. (2006) to explain part of the crustacean abundance increase during the SERIES experiment.

Only during some iron fertilisation experiments were the sampling gear and procedure adequate to resolve abundance in different depth strata and thus a vertical animal redistribution. Differences in the residence depth of non-diurnal and diurnal migrating copepods between inside and outside the phytoplankton bloom area were observed during IronEx II (Rollwagen Bollens & Landry 2000), EisenEx (Henjes et al. 2007), SERIES (Sastri & Dower 2006, Tsuda et al. 2006) and EIFEX (S. Krägefsky unpubl. data).

The migratory behaviour of *Oithona* spp. individuals can explain most of their abundance increase observed during EisenEx. These findings add to the increasing evidence that copepods are able to utilise vertical differences in current speed and direction to affect their drift for their own benefit, here in order to increase their food gain in a patchy food environment with a low background food concentration.

Acknowledgements. We thank J. Henjes for providing abundance data of *Oithona* spp. and B. Fach, H. Leach and 2 anonymous referees for valuable suggestions for improvement of the manuscript.

LITERATURE CITED

Anis A, Moum JN (1995) Surface wave-turbulence interactions: scaling ε(*z*) near the sea surface. J Phys Oceanogr 25:2025–2045

Assmy P, Henjes J, Klaas C, Smetacek V (2007) Mechanisms determining species dominance in a phytoplankton bloom induced by iron fertilization experiment EisenEx in the Southern Ocean. Deep-Sea Res I 54:340–384

Atkinson A (1995) Omnivory and feeding selectivity in five copepod species during spring in the Bellinghausen Sea, Antarctica. ICES J Mar Sci 52:385–396

Atkinson A (1996) Subantarctic coepepods in an oceanic, low chlorophyll environment: ciliate predation, food selectivity and impact on prey populations. Mar Ecol Prog Ser 130: 85–96

Atkinson A (1998) Life cycle strategies of epipelagic copepods in the Southern Ocean. J Mar Syst 15:289–311

Bainbridge R (1953) Studies on the interrelationships of zooplankton and phytoplankton. J Mar Biol Assoc UK 32: 385–447

Bakker DCE, Bozec Y, Nightingale PD, Goldson L and others (2005) Iron and mixing affect biological carbon uptake in SOIREE and EisenEx, 2 Southern Ocean iron fertilisation experiments. Deep-Sea Res I 52:1001–1019

Batchelder HP, Edwards CA, Powell TM (2002) Individual-based models of copepod populations in costal upwelling regions: implications of physiologically and evironmentally influenced diel vertical migration on demograhic success and nearshore retention. Prog Oceanogr 53: 307–333

Bosch HF, Taylor WR (1973) Diurnal vertical migration of an eustuarine cladoceran *Podon polyphemoides* in the Cheasapeake Bay. Mar Biol 19:172–181

Boyd PW, Jickells T, Law CS, Blain S and others (2007) Mesoscale iron enrichment experiments 1993–2005: synthesis and future directions. Science 315:612–617

Castellani C, Irigoien X, Harris RP, Lampitt RS (2005) Feeding and egg production of *Oithona similis* in the North Atlantic. Mar Ecol Prog Ser 288:173–182

Cisewski B, Strass VH, Prandke H (2005) Upper-ocean vertical mixing in the Antarctic Polar Front Zone. Deep-Sea Res II 52:1087–1108

Emsley SM, Tarling GA, Burrows MT (2005) The effect of vertical migration strategy on retention and dispersion in the Irish Sea during spring-summer. Fish Oceanogr 14: 161–174

Gonzáles HE, Smetacek V (1994) The possible role of the cyclopoid copepod *Oithona* in retarding the flux of zooplankton faecal material. Mar Ecol Prog Ser 113:233–246

Hardy AC, Gunther ER (1935) The plankton of the South Georgia whaling grounds and adjacent waters, 1926–1927. Discov Rep 11:1–456

Henjes J, Assmy P, Klaas C, Verity P, Smetacek V (2007) Response of microzooplankton (protists and small copepods) to an iron-induced phytoplankton bloom in the Southern Ocean (EisenEx). Deep-Sea Res I 54:363–384

Hopkins TL (1985) Food web of an Antarctic midwater ecosystem. Mar Biol 89:197–212

Hopkins TL (1987) Midwater food web in Mc Murdo Sound, Ross Sea, Antarctica. Mar Biol 96:93–106

Hopkins TL, Torres JJ (1989) Midwater food web in the vicinity of a marginal ice zone in the western Weddell Sea. Deep-Sea Res 36:543–560

Jansen S, Klass C, Krägefsky S, v. Harbou L, Bathmann U (2006) Reproductive response of the copepod *Rhincalanus gigas* to an iron-induced phytoplankton bloom in the Southern Ocean. Polar Biol 29:1039–1044

Kaartvedt S, Olsen E, Jørstad T (1996) Effects of copepod foranging behaviour on predation risk: an experimental study of the predatory copepod *Paraeuchaeta norvegica* feeding on *Acartia clausi* and *A. tonsa* (copepoda). Limnol Oceanogr 42:164–170

Kattner G, Albers C, Graeve M, Schnack-Schiel SB (2003) Fatty acid and alcohol composition of small polar copepods, *Oithona* and *Oncaea*: indication on feeding modes. Polar Biol 26:666–671

Kimmerer WJ, McKinnon AD (1987) Zooplankton in a marine bay. II. Vertical migration to maintain horizontal distributions. Mar Ecol Prog Ser 41:53–60

Klaas C (2001) Spring distribution of larger (>64 µm) protozoans in the Atlantic sector of the Southern Ocean. Deep-Sea Res I 48:1627–1649

Lampitt MR (1978) Carnivorous feeding by a small marine copepod. Limnol Oceanogr 23:1228–1230

Maar M, Visser AW, Nielsen TG, Stips A, Saito H (2006) Turbulence and feeding behaviour affect the vertical distributions of *Oithona similis* and *Microsetella norwegica.* Mar Ecol Prog Ser 313:157–172

Moore JK, Abbott MR (2002) Surface chlorophyll concentrations in relation to the Antarctic Polar Front: seasonal and spatial patterns from satellite observations. J Mar Syst 37: 69–86

Pasternak AF, Schnack-Schiel SB (2001) Feeding patterns of dominant Antarctic copepods: an interplay of diapause, selectivity, and availability of food. Hydrobiologia 453/454: 25–36

Peterson WT, Miller CB, Hituchinson A (1978) Zonation and maintenance of copepod populations in the Oregon upwelling zone. Deep-Sea Res A 26A:467–494

Rollwagen Bollens GC, Landry MR (2000) Biological response to iron fertilization in the eastern equatorial Pacific (IronEx II). II. Mesozooplankton abundance, biomass, depth distribution and grazing. Mar Ecol Prog Ser 201: 43–56

Sastri AR, Dower JF (2006) Mesozooplankton community response during the SERIES iron enrichment experiment in the subarctic NE Pacific. Deep-Sea Res II 53:2268–2280

Schnack-Schiel SB (2001) Aspects of the study of the life cycles of Antarctic copepods. Hydrobiologia 453/454:9–24

Shreeve RS, Ward P, Whitehouse MJ (2002) Copepod growth and development around South Georgia: relationships with temperature, food and krill. Mar Ecol Prog Ser 233: 169–183

Smetacek V, Scharek R, Nöthig EM (1990) Seasonal and regional variation in the pelagial and its relationship to the life history cycle of krill. In: Kerry K, Hempel G (eds) Antarctic ecosystems: ecological change and conservation. Springer Verlag, Berlin, p 103–114

Strass VH, Naveira Garabato AC, Pollard RT, Fischer HI and others (2002) Mesoscale frontal dynamics: shaping the environment of primary production in the Antarctic Circumpolar Current. Deep-Sea Res II 49:3735–3769

Strass V, Cisewski B, Gonzalez S, Leach H and others (2005) The physical setting of the European iron fertilisation experiment 'EIFEX' in the Southern Ocean. Rep Polar Mar Res 500:15–46

Svensen C, Kiørboe T (2000) Remote prey detection in *Oithona similis*: hydromechanical versus chemical cues. J Plankton Res 22:1155–1166

Tiselius P, Jonsson PR (1990) Foranging behaviour of six calanoid copepods: observations and hydromechanic analysis. Mar Ecol Prog Ser 66:23–33

Tsuda A, Saito H, Nishioka J, Ono T, Noiri Y, Kudo I (2006)

Mesozooplankton response to iron enrichment during the diatom bloom and bloom decline in SERIES (NE Pacific). Deep-Sea Res II 53:2281–2296

Uchima M, Hirano R (1988) Swimming behaviour of the marine copepod *Oithona davisae*: internal control and search for environment. Mar Biol 99:47–56

Visser AW (2001) Hydromechanical signals in the plankton. Mar Ecol Prog Ser 222:1–24

Voronina NM (1998) Comparative abundance and distribution of major filter-feeders in the Antarctic pelagic zone. J Mar Syst 17:375–390

Ward P, Hirst AG (2007) *Oithona similis* in a high latitude ecosystem: abundance, distribution and temperature limitation of fecundity rates in a sac spawning copepod. Mar Biol 151:1099–1110

Wend B (2005) Stage development of *Oithona similis* (Copepods: Cyclopoida) during EisenEx. Master's thesis, University Bremen

Wiggert JD, Haskell AGE, Paffenhöfer GA, Hofmann EE, Klinck JM (2005) The role of feeding behaviour in sustaining copepod populations in the tropical ocean. J Plankton Res 27(10):1013–1031

Woodson CB, Webster DR, Weissburg MJ, Yen J (2007) The prevalence and implications of copepod behavioral responses to oceanographic gradients and biological patchiness. Integr Comp Biol 91:1–16

Editorial responsibility: Hans Heinrich Janssen, Oldendorf/Luhe, Germany

Submitted: June 18, 2007; Accepted: October 1, 2008
Proofs received from author(s): December 3, 2008